Organic Process Research & Development **2000**, *4,* 357−361

On-Line Mid-IR Spectroscopy as a Real-Time Approach in Monitoring Hydrogenation Reactions

Ivan Marziano,* David C. A. Sharp, Peter J. Dunn, and Perry A. Hailey

Pfizer Central Research, Ramsgate Road, Sandwich CT13 9NJ, United Kingdom

Abstract:

The use of mid-IR spectroscopy as a real-time monitoring tool for hydrogenation reactions is illustrated. This technique was used for both qualitative and quantitative purposes to monitor the hydrogenation of three different functional groups. The results show that this technique can be successfully used as an alternative to traditional off-line methods to monitor the reaction endpoint and the formation of impurities.

Introduction

The use of on-line, real-time analytical techniques has been emerging in the last 10 years, both in R&D and in production environments.[1−3] A new analytical philosophy, termed process analytical chemistry (PAC), has been concomitantly developed. The principles of PAC are focused on the advantages of generating immediate analytical data to correct process deviations and eliminating the wait for the analytical response necessary to estimate the process status.[4] The most evident consequence of this approach is that, while classical analytical chemistry is aimed at simply providing information on the progress of a given step, PAC has also the objective of improving the overall process in terms of efficiency and costs.

On-line, real-time analytical techniques require no sample preparation and are generally non-invasive. Such techniques lend themselves particularly well to monitoring hydrogenation reactions. The traditional approach to monitoring these reactions involves cooling the reaction mixture, depressurising it, and collecting a sample, followed by analysis at a centralised analytical laboratory. Typically, analytical techniques such as HPLC, TLC, and NMR spectroscopy require a considerable period of time to provide an analytical response; during this period the reaction mixture is usually maintained at room temperature in the absence of hydrogen. On-line monitoring techniques provide an immediate result whilst eliminating the need for reaction depressurisation, thus preventing potential catalyst poisoning and considerably shortening the overall process time. Another, less obvious advantage is that some of these techniques can provide information on the unexpected accumulation of hazardous reaction intermediates. An example of this is the detection of potentially dangerous hydroxylamine intermediates in the reduction of nitro groups to amino groups.[5]

Two papers, both published in 1998, have discussed the use of various on-line techniques to monitor hydrogenation reactions in real time.[6,7] In one of the papers, the use of NIR spectroscopy in monitoring the conversion of an imino group to the *cis* and *trans* isomers of the corresponding amine was described.[6] In this example, the contributions to the spectral data arising from changes in the physical properties of the sample were eliminated by calculating the second derivative of the spectra acquired. Such data treatment highlighted variations ascribed to the first overtones N−H and C−H stretches. Further data exploration involved the use of principal component analysis (PCA) on the derivatised data, and then partial least squares (PLS) were successfully used to build a predictive model on a calibration set. The second paper described the simultaneous use of several in situ monitoring techniques during the hydrogenation of the nitro functionality in 1-(4-nitrobenzyl)-1,2,4-triazole and of the pyrazine ring to the corresponding piperazine functionality in pyrazine-2-*tert*-butylcarboxamide.[7] The techniques employed were reaction calorimetry, measurement of the hydrogen uptake, and on-line mid-IR spectroscopy. It was emphasised that real-time monitoring tools are a source of information on differential properties of the reaction mixture which can be used as the basis for mechanistic and kinetic studies.

This work describes the use of on-line mid-IR spectroscopy to monitor the hydrogenation of various functional groups. This technique was preferred to the other real-time techniques for the following two reasons:

(i) Direct information can be obtained without the necessity to treat the data with chemometric approaches (an advantage over NIR spectroscopy).

(ii) It provides information which can be specifically related to each component rather than the reaction mixture as a whole (an advantage over reaction calorimetry and hydrogen uptake measurement).

The spectral data were employed to measure and compare reaction rates within an experimental design set, to identify the presence of unwanted reaction by-products, and to build a predictive model to quantify the amount of unreacted starting material.

(1) Bortolotti, M.; Viola, T. G. *Polym. Prepr. (Am. Chem. Soc., Div. Polym. Chem.*) **1996**, *37*, 718−719.
(2) Cook, K. D.; Bennett, K. H.; Haddix, M. L. *Ind. Eng. Chem. Res.* **1999**, *38*, 1192−1204.
(3) Jaurich, O. *LaborPraxis* **1999**, *23*, 24−25.
(4) Hailey, P. A.; Doherty, P.; Tapsell, P.; Oliver, T.; Aldridge, P. K. *J. Pharm. Biomed. Anal.* **1996**, *14*, 551−559.
(5) Tong, W. R.; Seagrave, R. L.; Wiederhorn, R. *Loss Prev.* **1977**, *11*, 71−75.
(6) Ward, H. W., II; Sekulic, S. S.; Wheeler, M. J.; Taber, G.; Urbanski, F. J.; Sistare, F. E.; Norris, T.; Aldridge, P. K. *Appl. Spectrosc.* **1998**, *52*, 17−21.
(7) Le Blond, C.; Wang, J.; Larson, R.; Orella, C.; Sun, Y.-K. *Top. Catal.* **1998**, *5*, 149−158.

10.1021/op000030m CCC: $19.00
Published on Web 08/31/2000

Scheme 1. **Synthesis of B from A, involving the catalytic reduction of a nitro group**

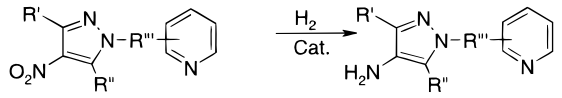

Scheme 2. **Formation of the by-product C from the reduction of the pyridine group in B**

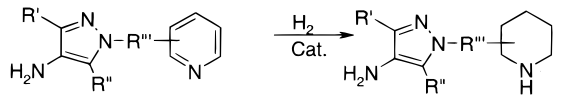

Experimental Section

The mid-IR spectra were acquired using a ReactIR MP spectrophotometer (ASI Applied Systems, Annapolis, MD) and a DiComp Attenuated Total Reflectance (ATR) probe (also obtained from ASI Applied Systems). The spectrophotometer was enclosed in an explosion-proof purged enclosure (CENELEC EN50.016.Eexp IIc T4) and connected to a control station located in an adjacent preparation room by means of modem twisted pair fibre optics. The spectral range was 4000−650 cm^{-1} (although the region between 2250 and 1950 cm^{-1} is affected by diamond absorbance of the Dicomp probe), and each spectrum was measured against an air background. The ATR probe was directly immersed into the reaction mixture, and spectra were automatically acquired at regular intervals throughout each reaction.

The predictive model for the conversion of **F** to **G** (see below) was generated using Microsoft Excel.

Information on reaction conditions is contained below in the individual reaction discussions.

Results and Discussion

(a) Hydrogenation of a Nitro Group to the Corresponding Amino Group in the Presence of a Pyridine Group. This series of reactions involved the catalytic reduction of a nitro group to the corresponding amino moiety. A schematic representation of the reaction is shown in Scheme 1.

It was observed that, in certain conditions, the product **B** was contaminated by substantial amounts of a by-product arising from the full reduction of the pyridine moiety (Scheme 2).

The objective of this series of experiments was to qualitatively monitor the formation of both the product **B** and the by-product **C**. A further objective was to minimise the reaction time (measured directly from the mid-IR spectral data) by identifying a set of optimal experimental conditions. To accomplish this goal, a series of several experiments was performed within an experimental design set.

Prior to the commencement of the experiments, mid-IR spectra of the starting material, the product, and the by-product were acquired. Some absorption bands characteristic for each of the three species were subsequently identified, and these are listed in Table 1.

Table 1. **Characteristic absorbance peaks observed during the synthesis of B**

peak wavenumber (cm^{-1})	assignment
1596	$-NH_2$ deformation
1509	$-NO_2$ asymmetric stretch
826	$-NO_2$ scissors (**A** only)
789	$-NH_2$ wagging (**B** and **C** only)
758	pyridine C−H wagging (**A** and **B** only)

A plot of the peak height at 1596 cm^{-1} (assigned to the $-NH_2$ deformation in the product **B**) and 1509 cm^{-1} (attributed to the $-NO_2$ asymmetric stretch in the starting material **A**) versus reaction time is shown in Figure 1. The profile for the peak at 1509 cm^{-1} shows the dissolution and then the reaction of the starting material. Corresponding to the decrease in this absorbance, an increase in the product peak at 1596 cm^{-1} was observed. Such profiles can be used to monitor the course of each reaction, with the endpoint defined as the point where the absorbances of both starting material and product have reached a constant level.

None of the spectral absorptions observed could be attributed to the presence of the by-product **C**. For example, the most intense mid-IR absorptions for a piperidine group (3280−3200 cm^{-1} for the N−H stretching and 3000−2760 cm^{-1} for the C−H stretching mode)[8] in this case would be masked by absorptions arising from the reaction matrix. However, the formation of this compound was monitored from the decrease in the intensity of an absorption peak at 758 cm^{-1}, corresponding to the wagging of C−H atoms of the pyridine group. The absorbance profiles at 758 cm^{-1} for two experiments which generated very different amounts of the impurity are shown in Figure 2.

(b) Catalytic Debenzylation. The debenzylation reaction schematically represented in Scheme 3 was performed with a 5% Pd/C catalyst and NaOH in the presence of H_2.

For this reaction, the solubility of the starting material **D** in the reaction solvent was very low, hence weak mid-IR spectral bands were observed. The product **E**, however, was highly soluble in a basic aqueous medium, and hence the appearance of several new absorption bands was observed throughout the reaction. Table 2 lists some functionalities present in both **D** and **E** and the corresponding mid-IR spectral absorbances. Such functionalities include heterocyclic rings present in the R group.

Other bands were observed only when **E** was present in solution, and these bands provided the best monitoring tools for the reaction. For example, Figure 3 shows a profile of absorbance at 1104 cm^{-1} (attributed to the asymmetric phosphate stretching), indicating an increase of the absorbance at this wavenumber, which corresponds to the product formation, up to a constant level after the reaction end. Such an absorbance plot was used to determine both the reaction endpoint and the relative reaction rates when reactions were performed using different experimental conditions.

(8) Lin-Vien, D.; Colthup, N. B.; Fateley, W. G.; Grasselli, J. G. *The Handbook of Infrared and Raman Frequencies of Organic Molecules*; Academic Press: London, 1991.

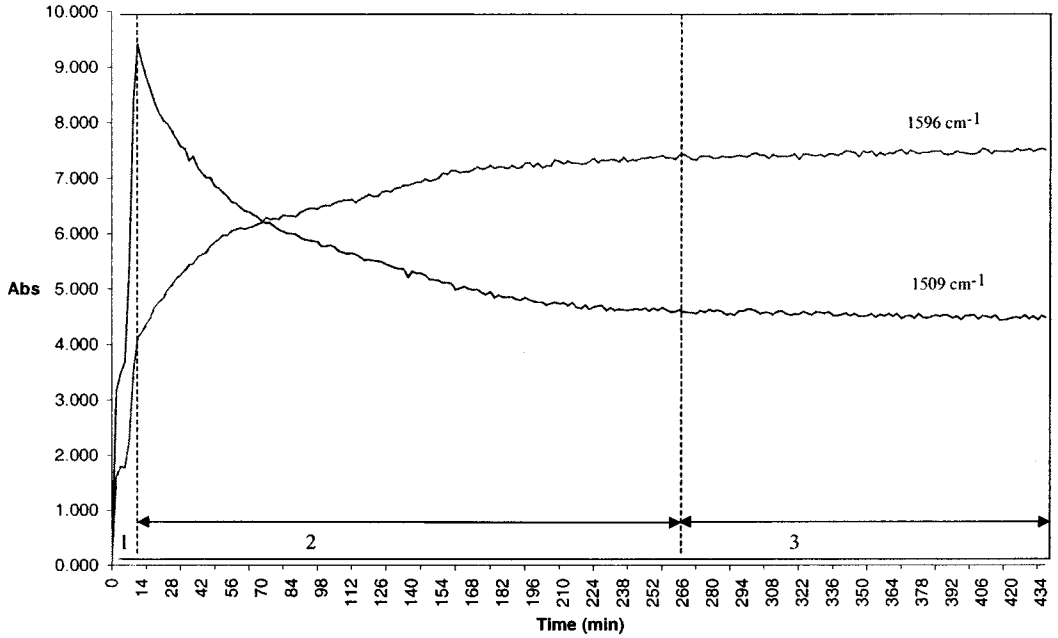

Figure 1. **Changes in absorbance at 1596 ($-NH_2$ asymmetric stretch) and 826 cm^{-1} ($-NO_2$ asymmetric stretch) plotted against the reaction time during the formation of B. 1: dissolution period; 2: reaction; 3: reaction completed.**

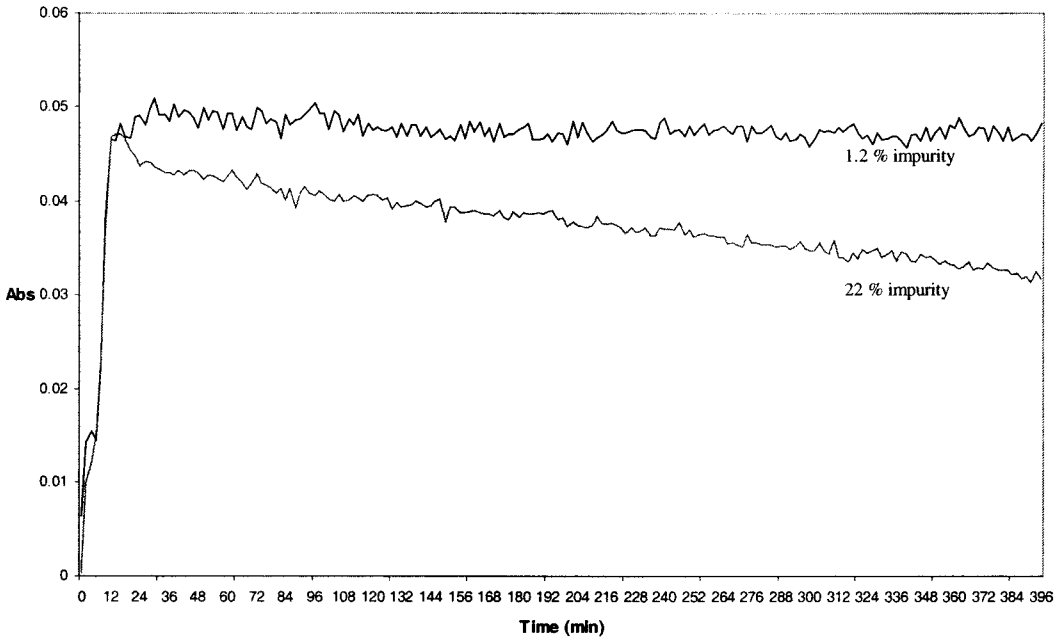

Figure 2. **Profiles of absorbances at 758 cm^{-1} (pyridine C−H wagging) vs reaction time for two different experiments resulting in different amounts of impurity.**

Scheme 3. **Synthesis of E from D, involving a catalytic debenzylation**

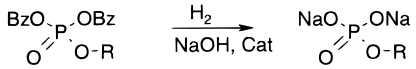

D E

(c) Reduction of a C═C Double Bond. The reaction shown in Scheme 4, involving the hydrogenation of a C═C double bond in the presence of 5% Pd/C, was investigated to determine whether the reaction could be monitored by mid-IR spectroscopy. Furthermore, the quantitative determination of the ratio of starting material **F** to product **G** was investigated using the same technique.

Table 2. **IR spectral absorptions from functionalities common to D and E**

functionality	wavenumber in **D**	wavenumber in **E**
heterocyclic ring stretching	1505	1501
out-of-phase P−O stretching	1275	1283
heterocyclic ring breathing	1138	1142

Four reactions were performed in total. Mid-IR spectra of the starting material **F** and the product **G** were acquired prior to the beginning of the reaction series to ascertain spectral differences between the two compounds. Absorption

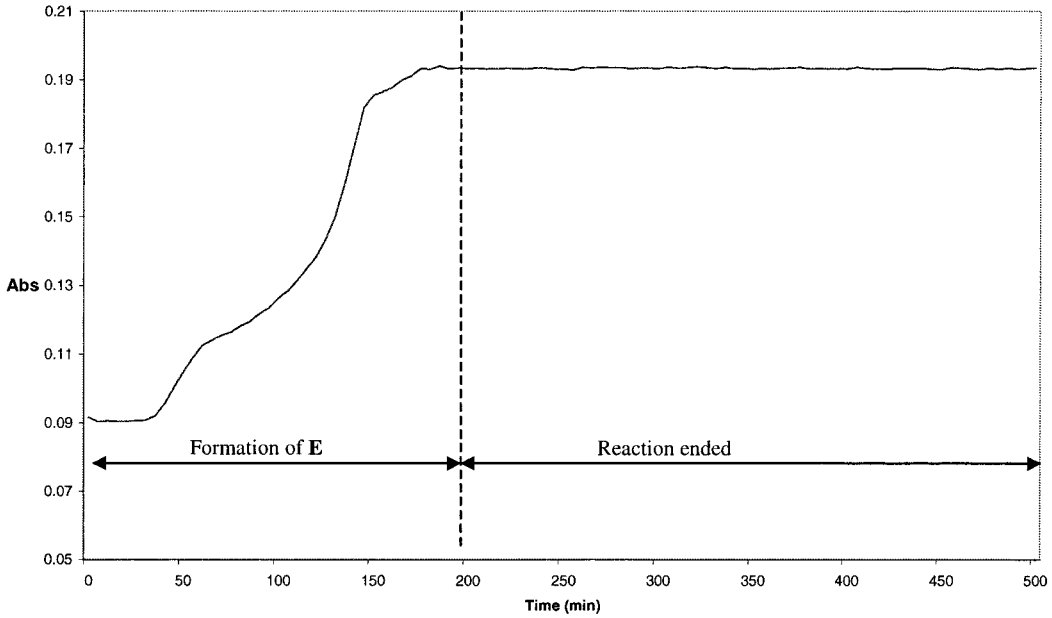

Figure 3. **Changes in absorbance vs time at 1104 cm^{-1} during the synthesis of E.**

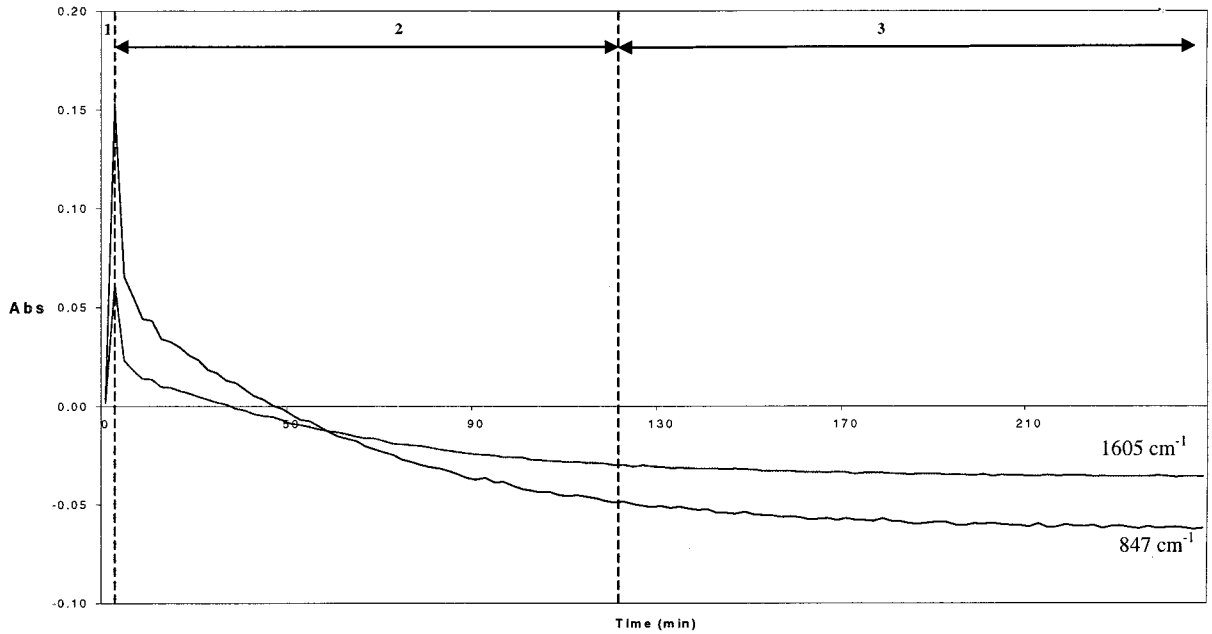

Figure 4. **Profiles of absorbance at 1605 and 847 cm^{-1}. 1: dissolution of F. 2: formation of G. 3: reaction completion.**

Scheme 4. **Synthesis of G from F, involving the reduction of a double bond**

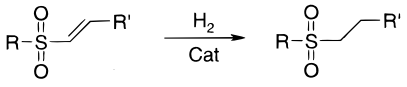

F G

peaks at 1605 and 847 cm^{-1}, assigned to the C═C stretch and the ─C═C─H deformation vibration respectively, were observed in **F** but not in **G**. During the first experiment, the reaction was monitored to determine whether changes in the absorbance at these two wavenumbers could be employed to identify the endpoint of the reaction. Shown in Figure 4 are profiles of absorbance versus reaction time at both wavenumbers, highlighting first the addition of the starting material **F** to the reaction medium, and then its conversion to **G**, with the reaction endpoint corresponding to the absorbances reaching a constant level.

During the remaining three experiments, the reaction mixture was sampled at regular intervals. This involved removing all H_2 from the reactor, purging the vessel with N_2, depressurising the vessel, collecting the sample, purging the vessel with N_2, and adding H_2 again. The samples were filtered and analysed by HPLC to provide the basis for a model to quantify the ratio of unreacted starting material **F** to product **G**. From the analysis of both HPLC and mid-IR spectral data, two important facts emerged: (i) a 4-fold increase in the reaction time was observed for the reactions during which sampling for HPLC analysis was performed, and (ii) a minimum of 2% of unreacted starting material was

Table 3. **Validation and predicted data for the polynomial model relating to the F/G ratio[a]**

test set peak area	actual ratio	predicted ratio	predicted − actual residuals
3.64	1.34	1.30	−0.04
3.49	0.73	0.73	0.00
3.34	0.34	0.36	0.02
3.25	0.15	0.20	0.05
3.07	0.02	0.06	0.04
3.46	0.69	0.65	−0.04
3.29	0.27	0.26	−0.01
3.06	0.04	0.06	0.02

[a] RMSEP is 0.034.

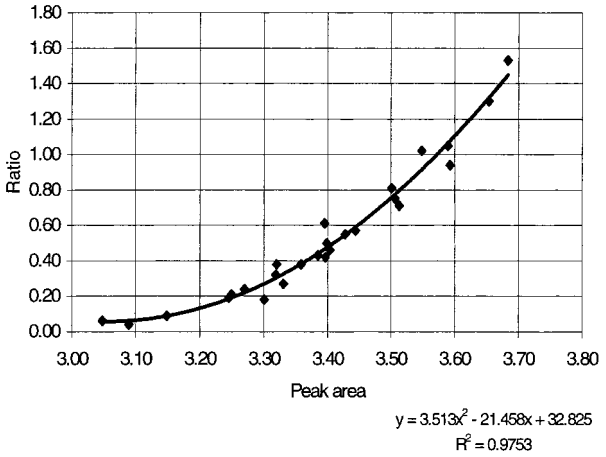

Figure 5. **Polynomial model for the fit of the peak area at 847 cm^{-1} vs F to G level with corresponding actual data points.**

observed at the end of each sampled reaction, in contrast with the first reaction, during which no sampling for HPLC analysis was performed and for which less than 0.4% of unreacted starting material was present at the end of the experiment. The latter is an important observation, underlining the effects of traditional sampling techniques on the process efficiency and the advantage of on-line analytical methods. Furthermore, these reactions were performed at room temperature, and the additional reaction time due to depressurising, sampling, and pressurising again cannot account for the extra process time observed, which was of the order of several hours.

The HPLC data and mid-IR spectral data were used to create a model to quantify the ratio of **F** to **G** on the basis of on-line IR spectral data. The data were analysed using both uni- and multivariate approaches. The best results were obtained when the peak area between 870.2 and 831.5 cm^{-1} (calculated to a single baseline point at 951.3 cm^{-1}) was used to build a prediction model for the starting material-to-product ratio. The best data fit was obtained with a second degree polynomial and when the predicted ratio was <1.6 (corresponding to a conversion of 38% or greater). The model was created from 26 data points from the three reactions data sets, and was validated using the remaining 8 data points. The validation set is shown in Table 3.

The equation representing the polynomial model employed for the regression is shown in Figure 5, along with a

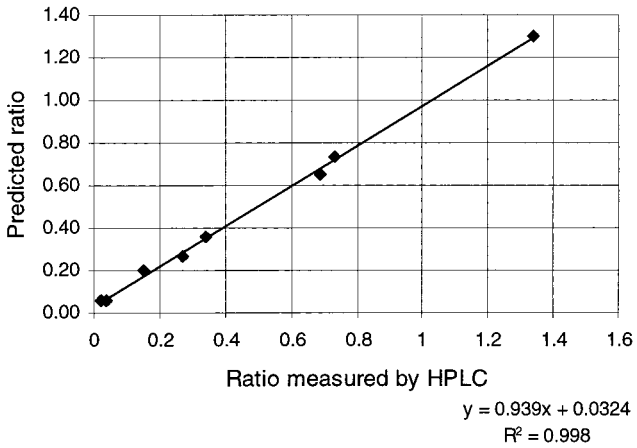

Figure 6. **The linear fit of the predicted vs the actual F to G level.**

plot of the peak area vs the ratio and the best-fit curve. The goodness-of-fit of the model on the calibration data was quantified by the related R^2 value (0.975).

Shown in Figure 6 is a plot of the predicted vs the actual **F** to **G** ratio, showing that the fit of the predicted data has a correlation R^2 of 0.998. The residuals are listed in Table 3.

This polynomial model can only be applied when the ratio of **F** to **G** is greater than 0.03, which corresponds to the minimum of the curve. Below this value the slope of the modelling curve is negative, and an increase in the ratio would be predicted when the peak area decreases below 3.05.

Conclusions

On-line mid-IR spectroscopy was successfully employed to monitor the hydrogenation reactions of several functional groups, to compare the relative reaction rates between runs, and to create quantitative models to determine the level of unreacted starting material.

In the case of one of the reactions, namely the reduction of a nitro group in the presence of a pyridine functionality, it was shown that the real-time determination of the reaction endpoint was crucial in preventing the formation of an unwanted over-reduction by-product.

Following this series of experiments, the hydrogenation of other functional groups will be investigated, with a further paper describing the results of these studies.

Acknowledgment

We thank John Deering and Trevor Newbury (Pfizer Central Research, Sandwich) for technical and scientific support. Sam Dunkerley (Pfizer Central Research, Sandwich) is thanked for helping with the data analysis. David am Ende and his team (Pfizer Central Research, Groton), who have also conducted studies of hydrogenation reactions using on-line spectroscopic techniques, are also thanked for useful discussions.

Received for review March 13, 2000.

OP000030M